Low-order chaos in sympathetic nerve activity and scaling of heartbeat intervals

Motohisa Osaka,[1,*] Hiroo Kumagai,[2] Katsufumi Sakata,[2] Toshiko Onami,[2] Ki H. Chon,[3] Mari A. Watanabe,[4] and Takao Saruta[2]

[1]*Department of Life Information Sciences, Institute of Gerontology, Nippon Medical School, 1-396 Kosugi, Nakahara-ku, Kawasaki 211-8533, Japan*

[2]*Department of Internal Medicine, Keio University School of Medicine, 35 Shinanomachi, Shinjuku-ku, Tokyo 160-8582, Japan*

[3]*Department of Electrical Engineering, City College of New York, New York, New York 10031*

[4]*Institute of Biomedical and Life Sciences, Glasgow University, Glasgow G12 8QQ, United Kingdom*

(Received 18 March 2002; revised manuscript received 13 January 2003; published 29 April 2003)

The mechanism of $1/f$ scaling of heartbeat intervals remains unknown. We recorded heartbeat intervals, sympathetic nerve activity, and blood pressure in conscious rats with normal or high blood pressure. Using nonlinear analyses, we demonstrate that the dynamics of this system of three variables is low-order chaos, and that sympathetic nerve activity leads to heartbeat interval and blood pressure changes. It is suggested that impaired regulation of blood pressure by sympathetic nerve activity is likely to cause experimentally observable steeper scaling of heartbeat intervals in hypertensive (high blood pressure) rats.

DOI: 10.1103/PhysRevE.67.041915 PACS number(s): 87.10.+e

I. INTRODUCTION

The power spectra of heartbeat intervals from healthy individuals exhibit a scale invariant $1/f$ pattern in the low-frequency range ($f<0.1$ Hz) [1–3]. Recent studies show that loss of this $1/f$ slope [4] and loss of heartbeat-interval multifractality [5] are closely correlated to the prognosis and severity of heart disease, but the mechanism underlying the heartbeat-interval power law scaling remains unknown [6,7]. Scale invariance is commonly associated with the chaotic dynamics, so nonlinearity in the dynamics of the system regulating heartbeat intervals would be a prime suspect. Physiologically, heartbeat intervals are determined by sympathetic nerve activity and blood pressure in a complex interaction that involves the brainstem and feedback loops, but the details of the interaction are unknown for low-frequency oscillations. One study has suggested that the low-frequency component of the heartbeat-interval power spectra is independent of sympathetic nerve activity [8]. However, we recently showed that the low-frequency blood pressure oscillations arise from sympathetic nerve activity, and that the elevated levels of sympathetic nerve activity in spontaneously hypertensive rats reduced the nonlinear correlation between sympathetic nerve activity and blood pressure that exists in normotensive (normal blood pressure) rats [9]. We therefore hypothesize that sympathetic nerve activity could also be responsible for the $1/f$ slope in heartbeat intervals and examine this hypothesis, using normotensive Wistar-Kyoto rats and spontaneously hypertensive rats [10]. The latter have higher sympathetic nerve activity, and are widely acknowledged to be an appropriate model of essential hypertension in man.

*Corresponding author. FAX: +81-44-733-1877; email address: osaka@nms.ac.jp

II. EXPERIMENTAL METHODS

The following is a brief description of our experimental methods. We used telemetry to record electrocardiograms [9]. The transmitter was implanted in the peritoneal cavity for 1 to 2 days before the experiment. The arterial pressure signal from a transducer attached to the left femoral artery catheter was amplified. Multifiber recordings of renal sympathetic nerve activity [11] were made from electrodes placed on the left renal nerve fascicle. Neural recording electrodes were connected to a high-impedance probe, which was connected to a differential amplifier with a band-pass filter of 50–1000 Hz. The filtered neurogram was integrated by a resistance-capacitance circuit (time constant=20 ms). Electrocardiogram, blood pressure, and renal sympathetic nerve activity were simultaneously recorded for over 100 min in conscious, unrestrained rats, both normotensive and spontaneously hypertensive (seven each). The signals were digitized with an analog-to-digital converter and sampled at 2 kHz. A smoothed instantaneous heart rate time series was constructed from heartbeat intervals between the *R* waves of the electrocardiogram using an algorithm proposed by Berger *et al.* [12]. The time series of heart rate, blood pressure, and renal sympathetic nerve activity were splined and sampled at 64 Hz, so that values of the entire constructed time series were made to occur simultaneously. To ensure accurate preservation of the low-frequency (<0.1 Hz) signals, we used a Butterworth filter, which lost no more than 0.5 dB in the passband <0.1 Hz and had at least 15 dB of attenuation in the stopband >0.15 Hz. We visually confirmed the absence of aliasing errors due to digitization and filtering.

III. MATHEMATICAL METHODS AND RESULTS

Figure 1 shows a typical heart-rate power spectrum from a normotensive rat plotted with log-log axes. Regression analysis was performed between 0.0005 and 0.02 Hz. In a similar manner to the power spectra in healthy humans [1,3],

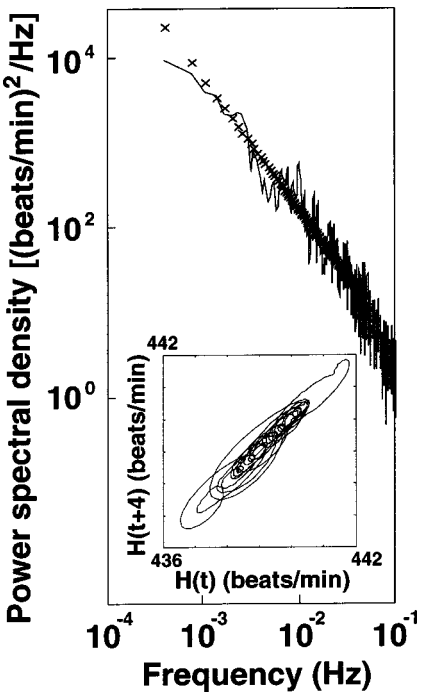

FIG. 1. Low-frequency portion of heart rate (beats/min) oscillation power spectrum from a normotensive rat. The crosses denote the regression line fitted over the range of 0.0005–0.02 Hz to the experimental data. Inset: Phase portrait.

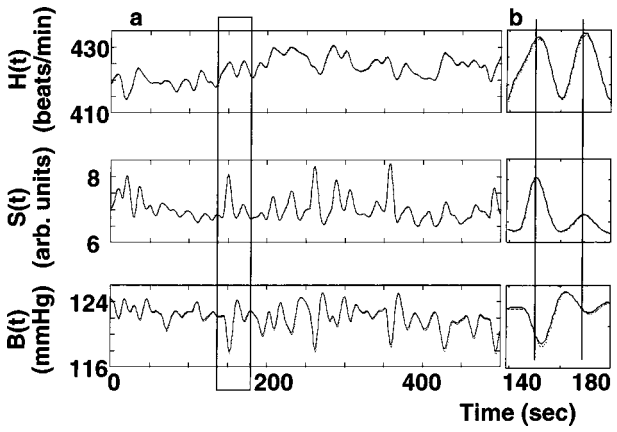

FIG. 2. (a) Filtered recording of heart rate $[H(t)$ (beats/min)], renal sympathetic nerve activity $[S(t)$ (arbitrary units)] and blood pressure $[B(t)$ (mmHg)] from the rat in Fig. 1 (solid line) and fit of a nonlinear autoregressive model (dotted line). The two lines are so close as to be indistinguishable. $S(t)$ and $H(t)$ share the same polarity and approximate timing of their extrema. Panel (b) shows the box in panel (a) on an expanded time scale. $S(t)$ peaks clearly precede $H(t)$ peaks and $B(t)$ nadirs.

the slope of the line fitted to the data is ≈ -1, indicating a $1/f$ relationship between frequency and power. The mean and standard error of the slope from normotensive rats was -1.35 ± 0.11 $(n=7)$. In contrast, the corresponding slope in spontaneously hypertensive rats was significantly greater, at -1.95 ± 0.12 $(n=7)$ $(p<0.05)$.

Several methods have been proposed to detect chaotic behavior in biological systems which tend to be noisy [13–15]. We used a recently developed algorithm [16], because it was the only method thought to be sensitive in cases where stochastic and deterministic components are both involved. This method first fits a nonlinear autoregressive model to a time series, followed by an estimation of the characteristic exponents of the model over the observed probability distribution of states for the system. More specifically, the model for a system output y can be written as

$$y_n = F[y_{n-1},\ldots,y_{n-k}] + k\varepsilon_n,$$

where F is a nonlinear (polynomial) function corresponding to the deterministic part, k is a constant, and ε_n are independent, identically distributed Gaussian random variables. The $k\varepsilon_n$ term corresponds to the stochastic part. We resampled the filtered heart rate, renal sympathetic nerve activity, and blood pressure data at 2 Hz $[H(t)$, $S(t)$, and $B(t)]$ and applied the above algorithm for data lengths of 500 s. The solid lines in Fig. 2(a) show a 500-s segment of $H(t)$, $S(t)$, and $B(t)$ recorded from a normotensive rat, the dotted lines, the result of the fit. The fit is remarkably accurate, considering that, for example, only 11 coefficients are needed to define 1000 points (500 s, 2 Hz) for the $S(t)$ trace in Fig. 2(a) (equation given in the Appendix). It must be noted, however, that the coefficients found for a particular data segment do not describe the coefficients for an adjacent data segment because the stochastic component brings about the sensitive dependence on initial conditions in this chaotic system (see below), resulting in rapid diversion from predicted values.

From the models, we obtained the characteristic exponents of the system by rewriting the model as a j-dimensional system, where j is the value of the largest delay in the model. The maximum dimension (delay) for any of the rats was low, at five. The largest Lyapunov exponents of $H(t)$, $S(t)$, and $B(t)$ were calculated for five random segments in each animal, and were always found to be positive, thereby indicating chaotic dynamics.

To find further evidence of low-order chaos, we constructed phase portraits in two-dimensional state space $[S(t)$, $S(t+T)]$. Plot α of Fig. 3 shows that some of the cycles in the phase portrait seem to have approximately the same period. Similarly, Fig. 2(b) shows cycles with a ~20-s period (0.05 Hz), and Fig. 1, cycles of 0.01, 0.005, and 0.002 Hz as well. We constructed stroboscopic plots of $[S(t)$, $S(t+T)]$ for an incident wave of 0.005 Hz. In plot α of Fig. 3 $(a-1)$ we can see stretching, folding, and compression, processes peculiar to low-order chaos. However, these processes were observed for 40 min at most, because the circulatory system was not being forced by a single oscillator at 0.005 Hz. Similarly, in plot β of Fig. 3 (incident wave of 0.002 Hz) and in plot γ of Fig. 3 (incident wave of 0.005 Hz) show evidence of determinism for $S(t)-H(t)$ and $S(t)-B(t)$ dynamics, respectively. The correlation dimensions of such phase portraits of $S(t)$ were also found to be low $(2.35\pm0.10$ in normotensive rats and 2.33 ± 0.10 in spontaneously hypertensive rats), another sign of chaotic dynamics. In summary, evidence for chaotic dynamics in the three-variable system consisted of continuous broad band power spectra, positive Lyapunov exponents, trajectories typical of low-

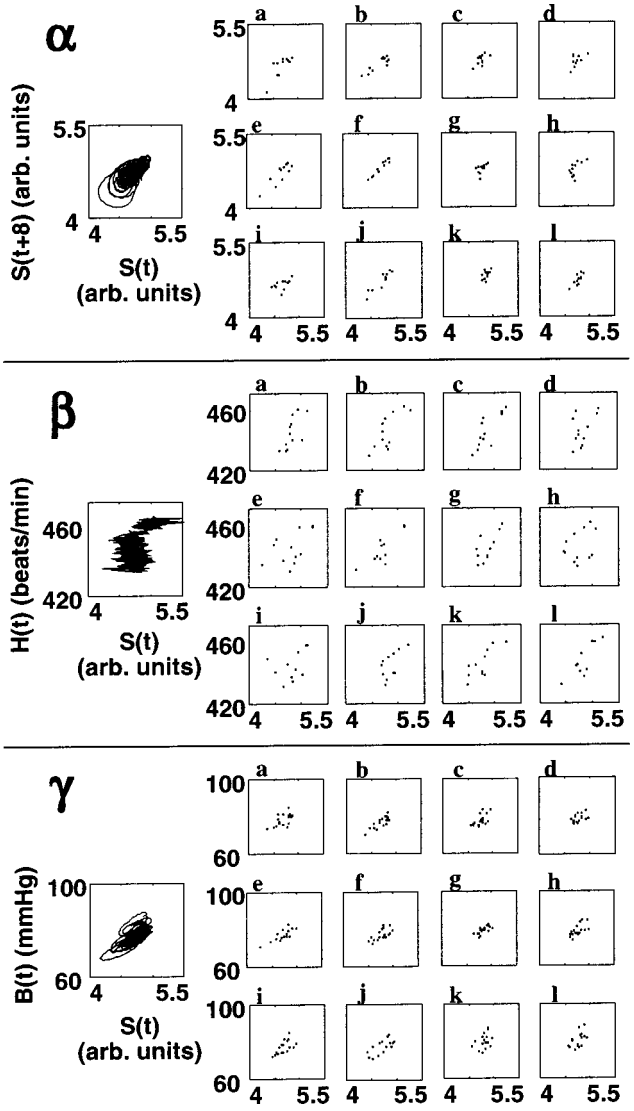

FIG. 3. Phase portraits and stroboscopic plots α, β, and γ of $[S(t),S(t+8)]$, $[S(t),H(t)]$, and $[S(t),B(t)]$. The phases of incident waves are from 0° to 330° with a step of 30°. $S(t)$, renal sympathetic nerve activity (arbitrary units); $H(t)$, heart rate; $B(t)$, blood pressure.

dimensional chaos, and phase portraits with a low number of correlation dimensions.

To analyze the correlation between sympathetic nerve activity and the other parameters, we calculated mutual information values between $S(t)$ and $H(t)$ and between $S(t)$ and $B(t)$, according to an algorithm proposed by Fraser and Swinney [17] and applied in our previous study [18]. Mutual information, to be defined precisely later, can be used for measuring the nonlinear as well as the linear dependence of two variables. For a pair of time series: $S=\{S(t)\}$ and $Q=\{Q(t)\}$, we measured how dependent the values of $Q(t+T)$ are on the values of $S(t)$. We made the assignment $[s,q]=[S(t), Q(t+T)]$ to consider a general coupled system (S, Q). The mutual information of this system $I(S, Q)$ is defined as the answer to the question, ''Given a measurement of a value s, how many bits on average can be predicted about a value q in probability?''

$$I(S, Q)=\int P_{sq}(s, q)\log[P_{sq}(s, q)/(P_s(s)P_q(q))]dsdq,$$

where (i) S and Q denote the systems, (ii) $P_s(s)$ and $P_q(q)$ are the probability densities at s and q, respectively, and (iii) $P_{sq}(s, q)$ is the joint probability density at s and q [17]. If the value of mutual information for (S, Q) is larger, it means that mutual dependence between S and Q is stronger. The data length of $S(t)$, $H(t)$, and $B(t)$ was 2^{13} (=8192), that is, 4096 s. Roulston has reported that for smaller datasets (<500), bias and random error can be a problem [19]. We therefore calculated mutual information values for datasets of length 8192. Because the algorithm was developed for a discrete case, mutual information values were normalized so that the values between 0 and 1 are independent of the data length. According to our previous study [18], a mutual information value of 0.047 is generally taken as the threshold value to discriminate correlated data from noncorrelated data. We calculated the mutual information $I(T)$ of (S, Q); S is a time series of renal sympathetic nerve activity and Q is another time series, $H(t+T)$ or $B(t+T)$, with a time delay T. T was then between -10 and 10 s in steps of 1 s. The maximum value of $I(T)$ between S and Q where T was from -10 to 10 s is denoted by $I_{\max}(S, Q)$. We considered the time delay $T_{\max}(S, Q)$, at which the maximum value of $I(T)$ of (S, Q) was given, as a physiological delay between these parameters [18]. If $T_{\max}(S, Q)$ is positive, it means that S leads Q. If $T_{\max}(S, Q)$ is negative, vice versa.

$I_{\max}(S, H)$ was 0.14 ± 0.06 and $I_{\max}(S, B)$ was 0.11 ± 0.05 $(n=7)$. The values of these data were clearly above threshold, indicating a strong correlation between sympathetic nerve activity and the other variables. This correlation is also observed in Fig. 2. Calculations showed that $S(t)$ led $H(t)$ by 1.1 ± 0.5 s and $B(t)$ by 1.5 ± 0.7 s $(n=7)$. This delay between sympathetic nerve activity and the other variables is also observable in Fig. 2(b) with the expanded time axis. In general, the $S(t)$ peaks precede the $H(t)$ peaks and $B(t)$ nadirs. We interpret this result as an indication that slow oscillations of heart rate and blood pressure are produced by slow oscillations of sympathetic nerve activity. The usual physiological interaction between blood pressure, heart rate, and sympathetic nerve activity is known as the baroreflex, wherein an increase (decrease) in blood pressure is compensated for by decrease (increase) in heart rate and vascular resistance, mediated by sympathetic nerve activity emanating from a reflex center in the brainstem. In other words, blood pressure drives sympathetic nerve activity. However, Figs. 2(a) and 2(b) show that $S(t)$ peaks precede peaks of $H(t)$ and nadirs of $B(t)$, which is consistent with a recent report that sympathetic nerve activity precedes blood pressure in conscious rats [9]. Thus, correlation in the low-frequency band (<0.1 Hz) is actually baroreflex independent. This bolsters the view that sympathetic nerve activity may play a causative role in hypertension. This hypothesis is supported by the observation that some of the nonlinear components of blood pressure regulation remain after baroreceptor denervation (neural incapability of monitoring blood pressure) [20]. The sympathetic nerve activity was significantly higher in our spontaneously hypertensive rats than in the normotensive

rats (16.1 ± 6.2 versus 7.2 ± 2.5 arbitrary units; $P<0.01$), despite their higher blood pressure (156 ± 17 versus 110 ± 7 mmHg; $P<0.001$). It seemed obvious that the interaction between sympathetic nerve activity and blood pressure might be impaired in spontaneously hypertensive rats, and that this might also cause the $1/f$ slope to be steeper.

IV. CONCLUSIONS

Spontaneously hypertensive rats, an animal model for human hypertension, have steep scaling of the low-frequency portion of their heartbeat-interval power spectra. Application of a nonlinear autoregressive algorithm shows that, hypertensive or not, low-frequency heartbeat-interval power spectra characteristics are determined by the low-dimensional chaotic dynamics of a system of three variables, heartbeat intervals, blood pressure and sympathetic nerve activity, that is different from interactions between the variables at higher frequencies (baroreflex). It is suggested that decreased sensitivity of blood pressure to sympathetic nerve activity is the cause of the steep scaling seen in the hypertensive animals.

ACKNOWLEDGMENTS

We thank Sunao Murashige and the other attendees at "Creation and Sustenance of Diversity—To Explore a New Theory of Diversity of Complex Systems," held at the International Institute of Advanced Studies at Kyoto, for helpful discussions. We also thank C. W. P. Reynolds for linguistic assistance with the manuscript.

APPENDIX

For example, the model equation for renal sympathetic nerve activity in Fig. 2(a) is as follows:

$$\begin{aligned} S(t) = {} & 1.8306S(t-1) + 0.2496S(t-2) - 1.5032S(t-3) \\ & - 0.0781S(t-4) + 0.5007S(t-5) \\ & - 0.1178S(t-1)S(t-1) + 0.3873S(t-1)S(t-2) \\ & + 0.011\ \ S(t-1)S(t-4) - 0.4232S(t-2)S(t-2) \\ & + 0.2139S(t-3)S(t-3) \\ & - 0.0711S(t-3)S(t-5). \end{aligned}$$

[1] M. Kobayashi and T. Musha, IEEE Trans. Biomed. Eng. **29**, 456 (1982).
[2] C. K. Peng *et al.*, Phys. Rev. Lett. **70**, 1343 (1993).
[3] J. P. Saul *et al.*, *Computers in Cardiology* (IEEE Computer Society, Silver Spring, MD, 1987), p. 419.
[4] J. T. Bigger *et al.*, Circulation **93**, 2142 (1996).
[5] P. C. Ivanov *et al.*, Nature (London) **399**, 461 (1999).
[6] A. L. Goldberger *et al.*, Biophys. J. **48**, 525 (1985).
[7] R. G. Turcott and M. Teich, Ann. Biomed. Eng. **24**, 269 (1996).
[8] J. Koh *et al.*, J. Physiol. (London) **474**, 483 (1994).
[9] K. Sakata *et al.*, Circulation **106**, 620 (2002).
[10] Y. Yamori, *Handbook of Hypertension* (Elsevier Science, Amsterdam, 1994), Vol. 16, p. 346.
[11] H. Kumagai *et al.*, Circ. Res. **67**, 1309 (1990).
[12] R. D. Berger *et al.*, IEEE Trans. Biomed. Eng. **33**, 900 (1986).
[13] L. Glass, Nature (London) **410**, 277 (2001).
[14] G. Sugihara and R. M. May, Nature (London) **344**, 734 (1990).
[15] X. Pei and F. Moss, Nature (London) **379**, 618 (1996).
[16] K. Chon *et al.*, Physica D **99**, 471 (1997).
[17] A. M. Fraser and H. L. Swinney, Phys. Rev. A **33**, 1134 (1986).
[18] M. Osaka *et al.*, Am. J. Physiol. **275**, H1419 (1998).
[19] M. S. Roulston, Physica D **125**, 285 (1999).
[20] C. D. Wagner *et al.*, Am. J. Physiol. **269**, H1760 (1995).